Linearity of Pulse Excited Coil-Less Fluxgate

Mattia Butta and Pavel Ripka

Czech Technical University, Prague 16627, Czech Republic

In this paper, we study the open-loop linearity of pulse excited coil-less fluxgate. Narrow current pulses can be used instead of classical sinewave for the excitation of the coil-less fluxgate. This method has shown several advantages, mainly regarding reduction of power consumption, normally in order of tens of microwatts. The disadvantage is that traditional phase-sensitive detection cannot be used as it results in a very small sensitivity. Using pulse excitation, the output signal is obtained by integrating a part of the positive pulse and a part of the negative pulse, and then summing up the resulting voltages. This process was realized using two boxcar averagers SR 4153. The achieved open-loop linearity error is much higher than for sinewave excitation and it is not sufficient for precise applications. We show that the linearity strongly depends on the symmetry of the two integrating windows. In order to obtain precise timing, we realized an excitation board using PIC microcontrollers, which provides both the pulsing signals for excitation current and the gating signals for integration. Using this board and optimum position of the integrating window, we obtained a 0.6% maximum nonlinearity in $\pm$100-μT range, which is sufficient for portable compass.

Index Terms—**Coil-less fluxgate, fluxgate, linearity, magnetic sensors.**

I. Introduction

COIL-LESS fluxgates are a particular type of orthogonal fluxgate sensor composed just of a magnetic microwire without any coils [1]. They are similar to "nonlinear giant magneto-impedance (GMI)" sensors [2], [3], but they work at lower frequencies (typically 10 kHz) and they use phase-sensitive detector to obtain linear characteristics. Moreover, they differ on the working principle [4]. First, coil-less fluxgates were excited by a sinewave current flowing into the microwire, which creates a circumferential excitation field $H_{\rm ex}$. If $H_{\rm ex}$ is high enough, periodical saturation will occur in circumferential direction. The voltage measured on wires $V_{\rm wire}$ terminations includes a resistive component and an inductive component, due to the varying circumferential flux. In case of saturation, fluxgate effect occurs when we apply longitudinal magnetic field, if the microwire has helical anisotropy. Fluxgate effect results in a shifting of the circumferential B–H loop given by longitudinal external field. In time domain, this corresponds to shifting in opposite direction of the peaks in $V_{\rm wire}$, corresponding to the rising and falling edges of the B–H loop.

The asymmetry of $V_{\rm wire}$ so determined has as a result the rising of even harmonics in the spectrum of $V_{\rm wire}$. This is different from "fundamental mode" fluxgate, which cannot distinguish between the field-dependent signal and resistive component coupled from the excitation [5]. Thus, fundamental mode fluxgate cannot be used in coil-less modification, although in some cases it may have lower noise than the classical second harmonic fluxgate [6].

II. Pulse Excitation

Despite the fact that sinewave excitation and even harmonic extraction were useful techniques to characterize the working principle of the coil-less fluxgate, they have shown to be an unfeasible way to achieve good performances in practical applications. This is due to high-power consumption and problematic implementation of harmonic extraction. Therefore, we have experimented excitation of the magnetic microwire by short pulses of current [7]. This allows us to achieve deep saturation (vital condition for any type of fluxgate), reducing the root mean square (RMS) value of the current, and consequently, the power consumption of the sensor. We prefer this approach over using tubular type of core with more turns of the excitation winding [8] as we believe that the simplicity of our sensor is an advantage for future mass production in planar technology [9]. In our case, we used 60-mA peak current, with 10% duty cycle, resulting in sensor power consumption as low as 40 μW.

In this case, second harmonic extraction from $V_{\rm wire}$ is not the best solution as most of the information is at higher order harmonics. On the contrary, we implemented gated integration of $V_{\rm wire}$. This technique consists of performing analog integration of a small portion of both positive and negative peaks in $V_{\rm wire}$. Although this is basically a time-domain technique, our output is still an analog voltage, not time interval such as in [11] and [12]. In fact, we may consider our approach as a modification of phase-sensitive detection for arbitrary time window. Even more generalized approach is used in digital signal processing (DSP) magnetometers [12]–[14]. We believe this is the reason why we did not observed increased noise which is otherwise a common disadvantage of time-domain methods.

This operation was performed using boxcar averagers SR 4153; then, we summed the obtained output voltages. This method to extract signal output has shown to be useful replacement of harmonic extraction, in case of pulse excitation of coil-less fluxgate. Unfortunately, it did not show to have very good linearity.

The usual method to improve sensor's linearity is to use feedback compensation. This would require a coil around the coil-less fluxgate, to generate the compensation field. As the main advantage of such sensor is the lack of any coil, we tried to improve the open-loop linearity, in order to avoid any need to additional coil.

Manuscript received March 06, 2009. Current version published September 18, 2009. Corresponding author: M. Butta (e-mails: buttam1@fel.cvut.cz; mattia@butta.org).

Color versions of one or more of the figures in this paper are available online at http://ieeexplore.ieee.org.

Digital Object Identifier 10.1109/TMAG.2009.2024898

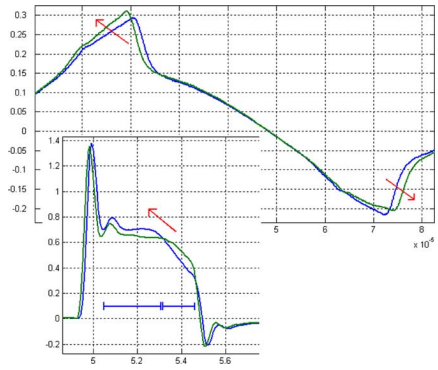

Fig. 1. Waveform of $V_{\rm wire}$ [V] versus [s] in case of 60-mA peak sinewave excitation (10 kHz). The shape differs when $\pm 50\ \mu$T is applied: peaks due to inductive voltage move in opposite direction. In the inset, the same situation is shown for pulse excitation (10% duty cycle). Due to the pulse shape, in the first range, the voltage increases, and after a knee (that is the point at $5.1 \cdot 10^{-5}$ s), it decreases.

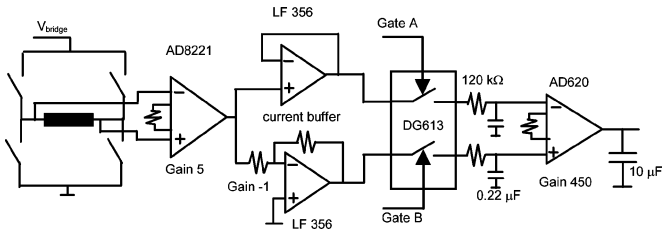

Fig. 2. Scheme of output signal extraction from $V_{\rm wire}$.

III. Source of Nonlinearity

The first step to improve the open-loop linearity of coil-less fluxgate is the identification of nonlinearity causes.

In order to do so, we must first understand how the gating integration method works. When the fluxgate effect occurs, the peaks in $V_{\rm wire}$ are shifted either to the right or to the left (Fig. 1). In case of pulse excitation, this results in deformation of $V_{\rm wire}$ waveform. In the inset of Fig. 1, we can identify two time ranges, before and after a knee (that is the intersection point at $5.1 \cdot 10^{-5}$ s). Before the knee, $V_{\rm wire}$ increases, whereas after the knee, it decreases (*vice versa* for the negative peak). If we select a slice of $V_{\rm wire}$ strictly included in one range (either before or after the knee) its integral will change due to the shifting of the peak.

The integral so obtained will be nonlinear even considering linear shift of the peak. This is due to the shape of the peak, which is not straight. The area under $V_{\rm wire}$ in the selected gating time for integration can change linearly only if it was a straight line moving either to the left or to the right. As this is not the case, the resulting integral will be nonlinear.

If we select the same gating interval for integration of opposite negative peak, we will obtain a second integral, which will not change linearly on shifting of the voltage peaks. However, we should notice that such nonlinearity is the opposite of the nonlinearity affecting the positive pulse (Fig. 3).

This is due to the fact that positive and negative peaks of the inductive component of $V_{\rm wire}$ are the result of the rising and falling edges of circumferential B–H loop. The longitudinal external field shifts such edges in the B–H loop, but it does not modify the loop's shape, which keeps symmetrical shape. The

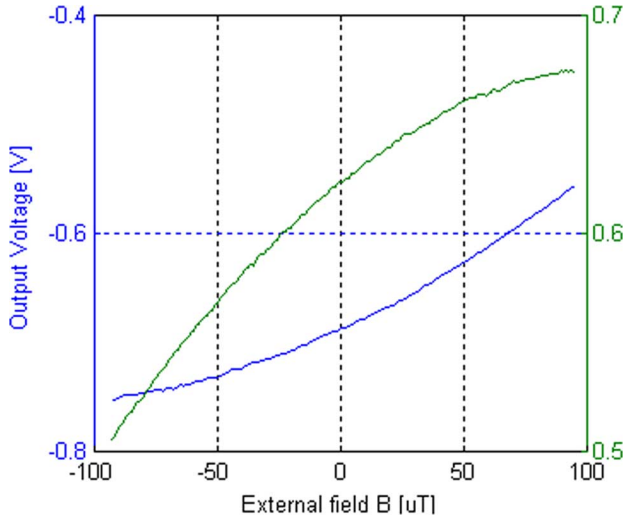

Fig. 3. Output voltages obtained by integrating only the negative peak (lower curve) or the positive peak (upper curve). They show strong nonlineaity.

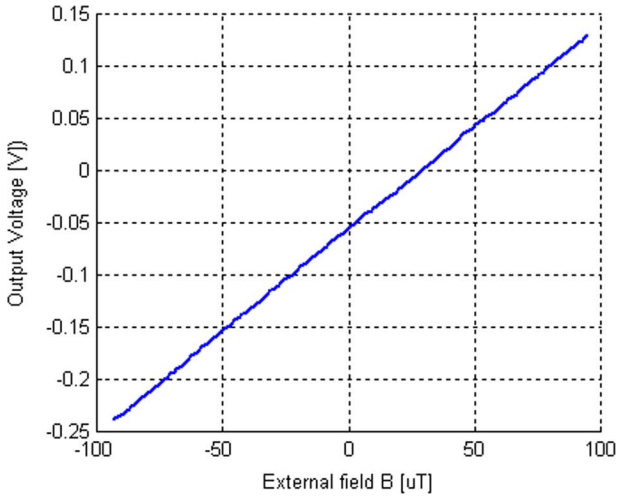

Fig. 4. Linear output characteristic obtained by integrating both positive and negative peak (Fig. 3). Nonlinearity of their integrals are mutually compensated for.

B–H loop symmetry sees that the nonlinearities of the positive and negative peaks integrals are mutually compensated for when they are summed up. This results in a linear characteristic (Fig. 4).

IV. Improvement of Linearity

Nonlinearity compensation between the integral of $V_{\rm wire}$ gated on positive and negative pulse works at best when the gating signals have exactly the same duration and they are exactly half period shifted. If the positive peak is integrated for a time longer than the negative peak, its integral will contain a part of nonlinearity, which cannot be compensated for by the integral of the negative pulse. That is why precise gating signals are important in order to obtain as much linear an output signal as possible.

As previously mention, we first used two box-car integrators/averagers SR 4153 to perform gating integration of $V_{\rm wire}$. These

devices have excellent performances in terms of speed and minimum duration of integrating time. Nevertheless, they do not allow the user to set the duration of the integrating time precisely enough. Therefore, we could not achieve identical gating time for both peaks, resulting in a degradation of final linearity.

In order to overcome this problem, we have developed an excitation board based on 16F737 PIC microcontroller, which provides better timing. The 16F737 has three independent pulse-width modulation (PWM) modules, here kept at constant duty cycle: one of them is used to generate the excitation signal, whereas the other two PWM signals are used to set the beginning and the end of integrating time. Thanks to a logic network, we split such signals both for positive and negative pulses. The board includes a 18F2550 PIC microcontroller as well, in order to provide USB connection to the PC. We developed a software which allows to change frequency, duty cycle, and amplitude of excitation pulses, as well as position and duration of the integrating window.

The employed PWM modules have 10-b resolution. This corresponds to ~50-ns resolution when generating 10-kHz exciting current. Such resolution is good enough to allow us to properly set width and position of gating signals. Such PWM modules use counter register, incremented by clock of the microcontroller central processing unit (CPU). Therefore, the only source of instability is given by the noise of the crystal used as clock source for the microcontroller. Frequency stability of employed crystal is ± 30 parts per million (ppm), good enough for our purpose.

Finally, we can assure that $V_{\rm wire}$ will be integrated over the same time both for positive and negative pulses, and any nonlinearity due to mismatch of gating signals will be avoided.

V. Signal Extraction

The voltage across wire terminations $V_{\rm wire}$ has been amplified by a AD8221 precision instrumentation amplifier, which provides a 700-kHz bandwidth for gain $= 5$, enough for the spectrum of the $V_{\rm wire}$ signal. We have compared the voltage resulting from this amplification stage with the voltage obtained using a Stanford Research amplifier SR 560, and we did not notice significant distortions. We did not increase the gain to higher values, to avoid saturation of the instrumentation amplifier (due to voltage peaks) as well as unacceptable reduction of bandwidth.

The amplified voltage is chopped by DG613 solid state switches, which have a 500-MHz bandwidth, low ON resistance (18 Ω), and maximum rising/fall time around 25 ns. Before the solid state switches, we have a current buffer. The negative pulse is inverted in order to switch a positive voltage, avoiding any asymmetry problem of positive and negative voltage power source at switches (then we had to subtract the integrals, instead of summing them, to fix back the sign).

Finally, we integrate the gated voltage signals by means by resistor/capacitor (RC) filter and AD620 instrumentation amplifier.

We tried to integrate only the positive pulse or only the negative pulse, to investigate the dependence of their integral on the applied filed. Fig. 4 shows the obtained output voltages in both cases (upper curve for positive pulse, and lower curve for negative pulse). We can see that they are strongly nonlinear, as expected from the theory previously exposed.

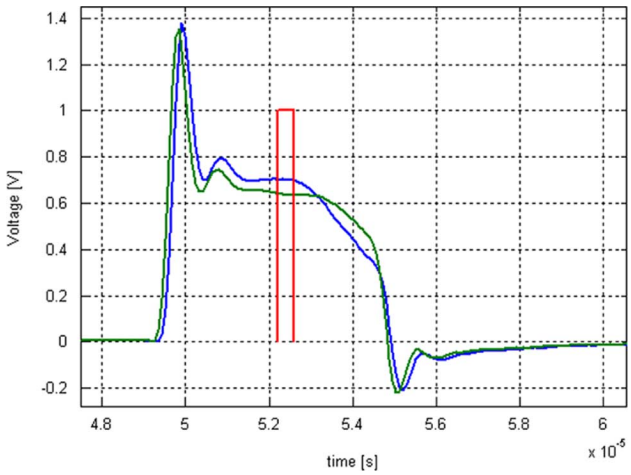

Fig. 5. Enlargement of positive peak of $V_{\rm wire}$ under application of $\pm 50\ \mu$T. Chosen gating pulse is shown. It has been selected in a time range where $V_{\rm wire}$ behaves monotonically.

However, when we integrate both signals coming from positive and negative pulses, we obtain a very linear characteristic (Fig. 4). This is due to the mutual compensation of the integrals shown in Fig. 3.

The obtained characteristic has ~2000 V/T sensitivity, and ± 100-μT linear range.

However, the most important feature we want to highlight is that we obtained good open-loop linearity: we have calculated 0.6% of full-scale maximum nonlinearity, which is enough for portable compass.

Linear range and signal sensitivity clearly depend on the selected position and width of the gating signal. The best results are achieved when the window is positioned in a time range when $V_{\rm wire}$ behaves monotonically. This condition is most easily achieved reducing the gate width, because the behavior of $V_{\rm wire}$ under application of the external field is as follows: the more uniform, the more one selects a short time range. On the other hand, the integration time cannot be reduced too much, as this brings an unacceptable reduction of sensitivity. Moreover, integration for a longer time compensates for the integration loss due to finite rise and fall time of the solid-state switch, and helps to reduce local noise of $V_{\rm wire}$ by averaging over a longer time.

In our case, we selected a 400-ns-long gating time, and we positioned it as shown in Fig. 5. This resulted in a low value of maximum nonlinearity, still providing a good sensitivity.

VI. Effect of Gating Signal Mismatch

As we have previously explained, the reason why we get a linear output characteristic lies in the mutual compensation of the integrals obtained by positive and negative gated pulses of $V_{\rm wire}$. This means that output linearity is not achieved by biasing the sensor in order to move the working point into the linear part of a nonlinear characteristic, as typically made for similar sensors. Such approach leads typically to poor stability of the sensor

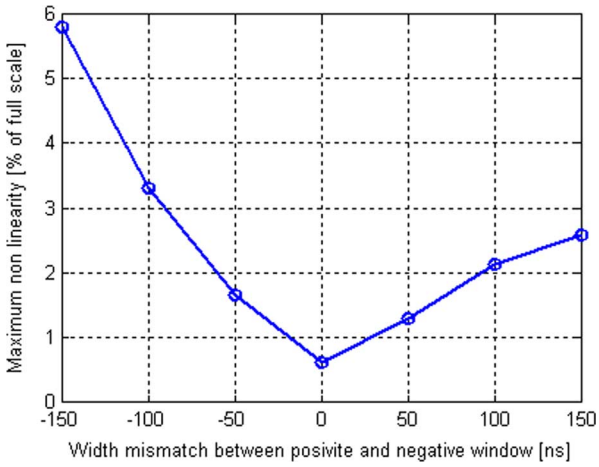

Fig. 6. Dependence of maximum nonlinearity (percent of full-scale) on the width mismatch between gating signal.

characteristics. In our case, the linearity lies in the structure and working mechanism of the coil-less fluxgate itself.

In order to verify our explanation, we have measured the output characteristic integrating only the positive pulse, and then we repeated the measurement with the negative pulse, increasing or reducing its duration in steps of 50 ns (time resolution). Finally, we numerically summed up the obtained integrals, in order to simulate the output characteristic with such mismatch between gating signals. Unfortunately, we had to do it numerically, because the electronic board cannot generate two gating signals with different width, but they are tied up to the same timing parameters by hardware structure.

Fig. 6 shows the result of our simulation of dependence of maximum nonlinearity on width mismatch between gating pulse. We can clearly see that even a small mismatch can really degrade the maximum nonlinearity. Let us consider a 25-ns mismatch, which is around 6% of the total time duration of the gating time (400 ns); it results in doubling the maximum nonlinearity form 0.6 % of full scale to 1.2 %.

This result highlights the necessity to have a precise match between gating signals, which cannot be achieved by manually setting duration of integrating time by analog knob on boxcar averager.

ACKNOWLEDGMENT

This work was supported by the research program MSM6840770015 “Research of Methods and Systems for Measurement of Physical Quantities and Measured Data Processing” of the Czech Technical University of Prague, Czech Republic, sponsored by the Ministry of Education, Youth and Sports of the Czech Republic.

REFERENCES

[1] M. Butta, P. Ripka, S. Atalay, F. E. Atalay, and X. P. Li, “Fluxgate effect in twisted magnetic wire,” *J. Magn. Magn. Mater.*, vol. 320, pp. e974–e978, 2008, DOI:10.1016/j.jmmm.2008.04.176.

[2] C. Gomez-Polo, M. Knobel, K. R. Pirota, and M. Vazquez, “Giant magnetoimpedance modelling using Fourier analysis in soft magneticc amorphous wires,” *Physica B*, vol. 299, pp. 322–328, 2001.

[3] S. Iida, O. Ishii, and S. Kambe, “Magnetic sensor using second harmonic change in magneto-impedance effect,” *Jpn. J. Appl. Phys.*, vol. 37, pp. L869–L871, 1998.

[4] M. Butta and P. Ripka, “Model for of coil-less fluxgate,” in *Proc. Eurosensors XXII Conf.*, Dresden, Germany, Sep. 7–10, 2008.

[5] I. Sasada, “Symmetric response obtained with an orthogonal fluxgate operating in fundamental mode,” *IEEE Trans. Magn.*, vol. 38, no. 5, pp. 3377–3379, May 2002.

[6] E. Paperno, “Suppression of magnetic noise in the fundamental-mode orthogonal fluxgate sens,” *Actuator A, Phys.*, vol. 116, pp. 405–409, 2004.

[7] M. Butta and P. Ripka, “Pulse excitation of coil-less fluxgate,” in *Proc. IEEE Sensors Conf.*, 2008, pp. 191–192.

[8] E. Paperno, E. Weiss, and A. Plotkin, “A tube-core orthogonal fluxgate operated in fundamental mode,” *IEEE Trans. Magn.*, vol. 44, pp. 4018–4031, 2009.

[9] O. Zorlu, P. Kejik, and R. S. Popovic, “An orthogonal fluxgate-type magnetic microsensor with electroplated Permalloy core,” *Sens. Actuators A*, vol. 135, pp. 43–49, 2007.

[10] B. Ando, S. Baglio, A. R. Bulsara, and V. Sacco, “V RTD fluxgate: A low-power nonlinear device to sense weak magnetic fields,” *IEEE Instrum. Meas. Mag.*, vol. 8, pp. 64–73, 2005.

[11] B. Ando, A. Ascia, S. Baglio, A. R. Bulsara, and J. D. Neff, “Towards an optimal readout of a residence times difference (RTD) fluxgate magnetometer,” *Sens. Actuators A*, vol. 142, pp. 73–79, 2008.

[12] E. B. Pedersen, F. Primdahl, J. R. Petersen, J. M. G. Merayo, P. Brauer, and O. V. Nielsen, “Digital fluxgate magnetometer for the Astrid-2 satellite,” *Meas. Sci. Technol.*, vol. 10, pp. N124–N129, 1999.

[13] W. Magnes, D. Pierce, A. Valavanoglou, J. Means, W. Baumjohann, C. T. Russell, K. Schwingenschuh, and G. Graber, “G: A sigma-delta fluxgate magnetometer for space applications,” *Meas. Sci. Technol.*, vol. 14, pp. 1003–1012, 2003.

[14] W. Magnes, M. Oberst, A. Valavanoglou, H. Hauer, C. Hagen, I. Jernej, H. Neubauer, W. Baumjohann, D. Pierce, J. Means, and P. Falkner, “Highly integrated front-end electronics for spaceborne fluxgate sensors,” *Meas. Sci. Technol.*, vol. 19, 2008, 115801.